Energy Equip. Sys./ Vol. 12/No. 3/September 2024/ 217-232

ENERGY EQUIPSYS

Energy Equipment and Systems

www.energyequipsys.com

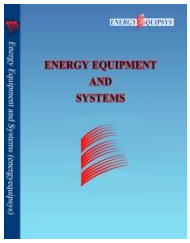

Effect of diamond-shaped turbolator on optimization of shell and tube heat exchanger

Manuscript Type
Research Paper

Authors

Hassan Hajabdollahi[a]
Sajjad Shamsi[a]
Mohammad Shafiey Dehaj[a*]

Department of Mechanical Engineering, Vali-e-Asr University of Rafsanjan, Rafsanjan, Iran

Article history:

Received : 21 January 2024
Revised : 5 February 2024
Accepted : 8 February 2024

ABSTRACT

In present study, the thermal modeling and multi-objective optimization of shell and tube heat exchangers (STHE) with a diamond-shaped turbulator has been investigated. To obtain the Correlation relationship between the Nusselt number and the friction factor for a diamond-shaped turbulator, a CFD analysis with acceptable accuracy has been done. Two factors of total cost and maximum thermal effectiveness are chosen as two objective functions. Nine optimal design variables for the present study are arrangement, diameter, step ratio, length and number of tube, distance ratio and cut ratio of baffle, turbulator step ratio and turbulator internal rod diameter. The ε-NTU procedure is employed for thermal modeling STHE and the Bell-Delaware technique is applied to evaluate the coefficient of heat transfer and pressure drop of the shell side. Also NSGA-II is used to acquire two objective functions. Comparison of the obtained results of the optimal Pareto optimal solutions showed that the use of diamond-shaped turbulator DST on the tube side improves thermal performance and lower overall costs STHE compared to the non-use state. Using turbulator inside the tube and the impact of important design parameters clearly contributed to the difference between effectiveness and overall cost.

Keywords: Heat Exchanger; Shell and Tube; Multi-Objective Optimization; Total Cost; Effectiveness.

1. Introduction

Nowadays, with the goal of energy saving, due to the constraints on energy resources, in order to optimize energy consumption, the production of heat exchangers (HEs) with higher efficiency and lower volume have found increasing attentions. HEs play a significant role in various engineering fields [1]. The optimization subject of HEs is multi-model in nature [2]. shell and tube heat exchangers (STHE) is one of the most usual HEs in the world due to high pressure resistance, high thermal resistance, easy construction, easy maintenance, robust construction and adaptability in operating conditions [3]. Petrochemical industries, power generation, food industries, environmental protection, waste thermal recovery, refrigeration and etc. are among the uses of this heat exchanger. In excess of 35-40% of the HEs employed in the world are of shell and tube type [4-6]. Heat increase enhancement methods can be used in

* Corresponding author: Mohammad Shafiey Dehaj
Department of Mechanical Engineering, Vali-e-Asr University of Rafsanjan, Rafsanjan, Iran
E-mail: m.shafiey@vru.ac.ir

three active, inactive and combining methods [7 and 8]. One of these inactive techniques to improve the effectiveness of the converter is the employing of turbulator inside the tube [9]. With the goal of improving thermal performance, increasing heat efficiency and reducing costs, modeling and optimization STHE has attracted many researchers. A Study of the research shows that Barus et al. [10] investigated Sustainability optimization of STHE, by applying a novel integrated methodology. It is moderately based on the employing of the "MIVES" method. Genetic algorithm methods and Monte Carlo simulation are used to maximize the stability index (SI). Their results showed Does not exist no relation with full-sized, strict sustainable development (SI = 1) Because various schemes have benefits and difficulties. Numerical investigation and optimization analysis of performance STHE in three modes (SG, CH and ST) is considered by Wang et al. [3]. They carried out a comparison of the heat transfer Operation and pressure drop between the three states STHE. They showed that Comprehensive performance STHE in state (ST) is premier to (CH) and (SG) modes. Van et al. [11] studied the Multi-parameter optimization of STHE with helical baffles. They founded that thermal resistance reduced with the velocity of the shell but enhanced with the spiral angle. Also, three optimized configurations were acquired by genetic algorithm that reduced thermal resistance by 7%. Van et al. [12] investigated to numerical research on the multi-objective optimization of a STHE with helical baffles. The results of their multi-purpose genetic algorithm (MOGA) showed that, with Comparison the original HE, the general coefficient of heat transfer enhanced by 28.3%, however the average pressure drop decreased by 19.37%. Wang et al. [13] investigated in study other configuration optimization STHE with helical baffles using NSGA based on fluid-structure interaction. They founded that the coefficient of heat transfer per unit pressure drop enhances averagely by 14.1% and the maximum shear stress reduces averagely by 4.1%. Tharakeshwar et al. [14] investigated Multi-objective optimization by bat algorithm for STHEs. Their results showed that the best solution (Pareto) of the bat algorithm reduced the cost by a maximum of 13.7% and a minimum of 9.2%. With cost reduction, the effectiveness rate fell by about 3%. Rao and Saroj [15] investigated the STHE optimization by employing Jaya algorithm with maintenance consideration. Their results showed the superiority of the Jaya algorithm in the newest described procedures for optimization and lack of similar problems with other algorithms. Mohanty [16] investigated the use of Firefly algorithm for optimization scheme of a STHE from economic point of view. He found that operating costs could be decreased by 77%, though the TOC could be decreased to 29% in comparison to the unique scheme. Also, the results of the Firefly algorithm represent a much better solution to the economic optimization problem for the design of a STHE. Techno-economic optimization of a STHE by GA and particle swarm algorithms Energy Conversion and Management studied by Sadeghzadeh et al. [17]. Comparison of their obtained results by two algorithms showed that the results obtained from the particle mass optimization technique are better to the GA methods. Hajabdollahi et al. [18] investigated the Thermo-economic optimization of a ST condenser by employing both GA and PSO. Their results showed that the genetic algorithm provides better results for the computer processor than the particle mass algorithm. Also, increasing the number of tubes initially cause a reduction in the objective function, and then caused to a significant increase in the objective function. Multi-objective optimization of STHE studied by Sanaye and Hajabdollahi [19]. Their results noticeably indicated the level of conflict between two objective functions. The effect of applying cone-shaped turbulator on heat transfer and friction factor inside the tube investigated by Eiamsa-ard et al. [20], experimentally. They indicated that the heat transfer rate enhances with the augmentation of Reynolds number and angle cone shape while decreases by augmentation of the ratio of the tail length. Naphon [21] studied the pressure drop and heat transfer in the horizontal double pipes with and without twisted tape insert. Their results showed that the insertion of the twisted band has a major influence on the increase of the heat transfer rate. However, the pressure drop also increases. Pourahmad and Pesteei [22] investigated the efficiency

analyses in a double tube HE furnished with wavy strip considering different angles. They developed some empirical correlations expressing the results based on curve fitting. Rao et al. [23] provided wide literature survey of different HEs for the ideal scheme by applying advanced optimization procedures concerning with different sides. They indicated that the parametric design optimization of HEs is related with number of structural and physical limitations. Saldanha et al. [24] comprehensively provided a state-of-the-art review of optimization by evolutionary computation techniques of STHE of single segmental baffles [24].

As it is observed, in the previous works, single and multi-objective optimization of different types of heat exchangers were performed considering different objective functions. In the presented work, diamond-shaped turbulator is used as an additional equipment to increase the rate of heat transfer. However, using this type of equipment increase the pressure drop in the base state as compared with the conventional exchanger. As a result, optimization process is required to show the advantage use of this type of turbulator.

As a summary the following are the contribution of this paper into the subject:

- Thermal modeling and multi-objective optimization of STHE with a diamond-shaped turbulator has been investigated.

- Nusselt number and the friction factor for this type of turbulator are approximated using CFD analysis with acceptable accuracy.

- Two factors of total cost and maximum thermal efficiency are chosen as two objective functions. - Nine optimal design variables including tube arrangement, tube diameter, tube pitch ratio, tube length, tube number, baffle spacing ratio as well as baffle cut ratio, turbulator step ratio and turbulator internal rod diameter are selected.

- Changes in optimal efficiency and total cost with changes in design variables STHE and sensitivity analysis have also been studied.

Nomenclature

$A_{o,t}$	tube flow area per crossing , m^2
A_t	total tube heat transfer area , m^2
A_s	flow area at near of the shell centerline , m
BC	baffle cut, m
C_P	specific heat, $J\ kg^{-1}K^{-1}$
C_{min}	minimum of C_h and C_c, WK^{-1}
C_{max}	maximum of C_h and C_c, WK^{-1}
C^*	heat capacity rate ratio, C_h/C_{max}
C_{in}	total investiture cost, \$
C_{op}	total operating cost, \$
C_o	yearly operating cost, \$ yr^{-1}
C_{total}	total cost, \$
CL	tube layout constant
CTP	tube count calculation constant
D_i	tube side inside diameter, m
D_o	tube side outside diameter, m
D_s	shell diameter, m
d_i	diameter of inner rod, m
d_o	diameter of turbulator, m
f	friction factor
h_i	tube side heat transfer coefficient, $W\ m^{-2}K^{-1}$
h_o	shell side heat transfer coefficient, $W\ m^{-2}K^{-1}$
i	yearly discount rate, %
j	Culburn number
k_w	thermal conductivity, $W\ m^{-1}K^{-1}$
K_C	entrance pressure loss coefficient
K_e	exit pressure loss coefficient
K_{el}	price of electrical energy, \$ $(kWh)^{-1}$
L	tube length, m
l	head length of D-shape turbulator, m
m	mass flow rate, $kg\ s^{-1}$
Nu	Nusselt number
Pr	Prandtl number
Q	heat transfer rate, W
Re	Reynolds number
L_{bc}	baffle spacing, m
ny	equipment life, yr
n_p	number of tube pass
N_t	number of tube
NTU	number of transfer units
p_t	tube pitch, m
P	pumping power, W
$R_{o,f}$	fouling resistance shell side, $m^2k\ W^{-1}$
$R_{i,f}$	fouling resistance tube side, $m^2k\ W^{-1}$
U	total heat transfer coefficient , W $m^{-2}k^{-1}$
S	Step, m
t	thickness of test tube, m
T	temperature, K
SR	Step ratio, $(S+l)/S$
u	mean axial velocity, $m\ s^{-1}$
$\dot{V}$	volume flow rate, $m^3\ s^{-1}$

Greek symbols

ϵ thermal effectiveness
ΔP Pressure drop, Pa
v kinematic viscosity, $m^2\ s^{-1}$
ρ density, $kg\ m^{-3}$
μ dynamic viscosity, $N\ s\ m^{-2}$
η_p pump efficiency
η enhancement efficiency
τ hours of operation per year, h/yr
σ ratio of minimum free flow area to frontal area

Subscripts

a air
b bulk
con convection
i inner or inlet
o outer or outlet
Pt plain tube
t tube side
s shell side
w tube wall

2. Thermal modeling

Various types of STHE have been used in engineering programs. E, F and K are different types of shells in the TEMA (Tubular exchanger manufacturing association) standard [25]. In this paper used E type. Figure (1) shows the typical single-pass STHE type E [26]. Also, with the definite input temperatures known, for the thermal modeling of effectiveness, the number of transmission units or the ε-NTU method has been used. The effectiveness term (NTU) for an E-type shell is written as:

$$\varepsilon = \frac{2}{\left(1+C^*\right)+\sqrt{\left(1+C^*\right)}\ \coth\left(\frac{NTU}{2}\sqrt{\left(1+C^*\right)}\right)} \quad (1)$$

In which the ratio of thermal capacity (C^*) and the number of transfer units (NTU) is cleared as (2 and 3):

$$NTU_{max} = \frac{U_0 A_t}{C_{min}} \quad (2)$$

$$C^* = \frac{C_{min}}{C_{max}} \quad (3)$$

In (2), A_t the overall heat transfer area in the external tube and U_0 is called the total heat transfer coefficient and is written in the form of relations (4 and 5) [25]:

$$A_t = \pi L d_o N_t \quad (4)$$

$$U_0 = \frac{1}{\frac{1}{h_o} + R_{o,f} + \frac{d_o \ln\left(D_o / D_i\right)}{2K_w} + R_{i,f}\frac{d_o}{d_i} + \frac{1}{h_i}\frac{d_o}{d_i}} \quad (5)$$

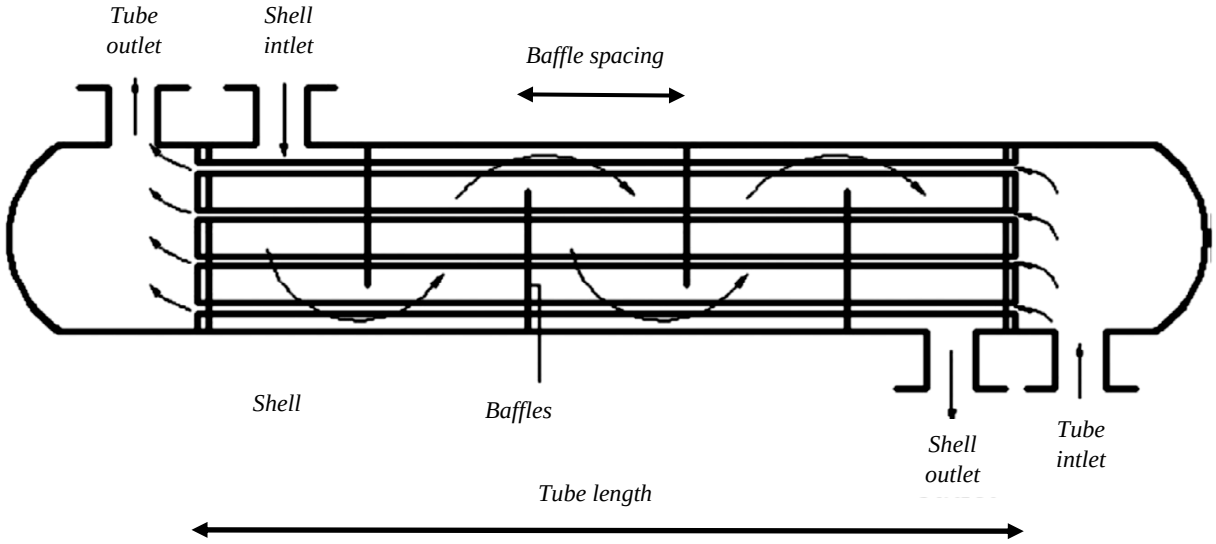

Fig. 1 Schematic diagram of a single-pass STHX.

2.1. Shell side

In present research, Belle-Delaware procedure is employed to evaluate and calculate heat transfer coefficient and pressure drop. According to this method, the heat transfer coefficient of the shell side is expressed in the form of relation (6) [27]:

$$h_o = h_s = h_{id} J_c J_l J_b J_s J_r \tag{6}$$

The correction factors J_c, J_l, J_b, J_s and J_r are selected with respect to the tube arrangement and the number of Reynolds. J_r, J_c, J_l, J_b and J_s are respectively the correcting factors for the adverse temperature gradient of laminar flow, baffle configuration, baffle leakage effects, flow crossing and larger baffle intervals in the inlet and outlet sections[25]. In the Belle-Delaware method, the ideal heat transfer coefficient for cross-flow in the tubes is gained and corrected by correction of some factors. The ideal heat transfer coefficient of the shell side is written as follows [27]:

$$h_{id} = j_s c_{p,s} \left(\frac{\dot{m}_s}{A_s}\right)\left(\frac{k_s}{c_{p,s}\mu_s}\right)^{2/3}\left(\frac{\mu_s}{\mu_{s,w}}\right)^{0.14} \tag{7}$$

where c_p, $\dot{m}_s$, k_s and μ_s are respectively the specific heat, mass flow rate, thermal conductivity coefficient, and viscosity of the shell side. Also $\frac{\mu_s}{\mu_{s,w}}$ is the shell viscosity ratio at wall temperature. A_s is the flow area at near of the shell centerline and j_s is the ideal Calibron factor of the shell side. A_s and j_s are calculated as relations (8 and 9) [27]:

$$A_s = \frac{D_s}{p_t}\left(p_t - d_o\right)BS \tag{8}$$

$$j_s = a_1\left(\frac{1.33}{p_t / d_o}\right)^{a}\left(Re_s\right)^{a_2} \tag{9}$$

where p_t is the tube step and BS is the baffle spacing. The reynolds number of the shell side and constant a are also expressed in the form of relations (10 and 11):

$$Re_s = \frac{d_o \dot{m}_s}{\mu_s A_s} \tag{10}$$

$$a = \frac{a_3}{1+0.14\left(Re_s\right)^{a_4}} \tag{11}$$

The constants $a_1 - a_4$ depend on the shape of the tube and the number of Reynolds and are obtained by the TEMA standard. The friction factor of the shell side follows from equation (12) [27]:

$$f_s = b_1\left(\frac{1.33}{p_t / d_o}\right)^{b}\left(Re_s\right)^{b_2} \tag{12}$$

$$b = \frac{b_3}{1+0.14\left(Re_s\right)^{b_4}} \tag{13}$$

The constants $a_1 - a_4$ depend on the shape of the tube and the number of Reynolds and are obtained by the TEMA standard. The diameter of the shell side is written in the form of relation (14):

$$D_s = 0.637\, p_t \sqrt{\left(\pi N_t\right) CL / CTP} \tag{14}$$

CL is a constant tube that has a unit value for arrangement 45 and 90° tube and 0.87 for arrangement 30 and 60° tube. Also, the CTP is tube count constant, which has a value of 0.93, 0.9 and 0.85, for single-pass, two-passes and three-pass pipes, respectively [27]. (ΔP_s) is the total pressure drop of the shell side. With the sum of the three cross-flow pressure drop (ΔP_{cr}), the pressure drop at the inlet and outlet (ΔP_{i-o}), and the window section pressure drop (ΔP_w), the total pressure drop of the shell side (ΔP_s) obtained as follow the relation (15):

$$\Delta P_s = \Delta P_{cr} + \Delta P_{i-o} + \Delta P_w \tag{15}$$

The details of how the pressure drop calculations, the Calibron factor, the friction coefficient, the cross flow area at or near the shell centerline of the shell and the constants (9, 11) and (12 and 13) are given in reference (12 and 13).

2.2. Tube side

2.2.1 Plain tube

First, the corresponding relationship for the tube side without DST (simple tube) is presented as follows, and then the relation for the tube with the DST is provided. The heat transfer coefficient h_t follows for the simple tube of (16) [25]:

$$h_t = \left(k_t / d_i\right) 0.024 Re_t^{0.8} Pr_t^{0.4} \quad \text{for} \quad 2500 < Re_t < 1.24\times10^5 \tag{16}$$

where k_t is the thermal conductivity coefficient of the tube side, Pr_t is the prantel number of the tube side and Re_t is the reynolds number of the tube side. The Reynolds number of the tube side is calculated as:

$$Re_t = \frac{d_i \dot{m}_t}{\mu_t A_t} \tag{17}$$

Here, also, $\dot{m}_t$ is the mass flow rate, and A_t, which is the area of the cross flow section of the pipe side, is written as [25]:

$$A_t = 0.25\,\pi {d_i}^2\, N_t / n_P \tag{18}$$

where n_P show the number of pass tube. The pressure drop of the tube side is also expressed as:

$$\Delta p_t = \frac{G^2}{2\rho_i}\left[\left(1-\sigma^2+K_{in}\right)+2\left(\rho_i/\rho_o-1\right)+\frac{4 f_t L}{d_i}\rho_i\left(1/\rho\right)_m-\left(1-\sigma^2+K_o\right)\rho_i/\rho_o\right] \tag{19}$$

where K_in is the pressure drop coefficient at the tube inlet and K_o is the pressure drop coefficient at the tube outlet.

The friction factor for the tube side is expressed as:

$$f_t = 0.00128 + 0.1143\left(Re_t\right)^{-0.311} \quad for \quad 4000 < Re_t < 10^7 \tag{20}$$

2.2.2. Tube with DST

In this study, DST was used as a passive method to increase heat transfer and its effect on objective functions (efficiency and total cost) on the tube side. In Fig. 2, the details of the study tube have been shown DST. The tube is made of copper and has a length of 1250 millimeters and a thickness of 1.5 millimeters. The inner diameter of the tube is 47.5 mm and the outer diameter is 50.5 mm. The DST material is made of stainless steel. The analyzed physics consists of an internal flow inside a copper tube in which a DST is made of stainless steel and causes turbulence in the fluid inside the tube. Parameters DST for simulation including step ratio (SR= 1.2 and 3), tube inside diameter (d_i= 3.6 and 9 mm) and Reynolds number, which varies in the range of 3500-16500.

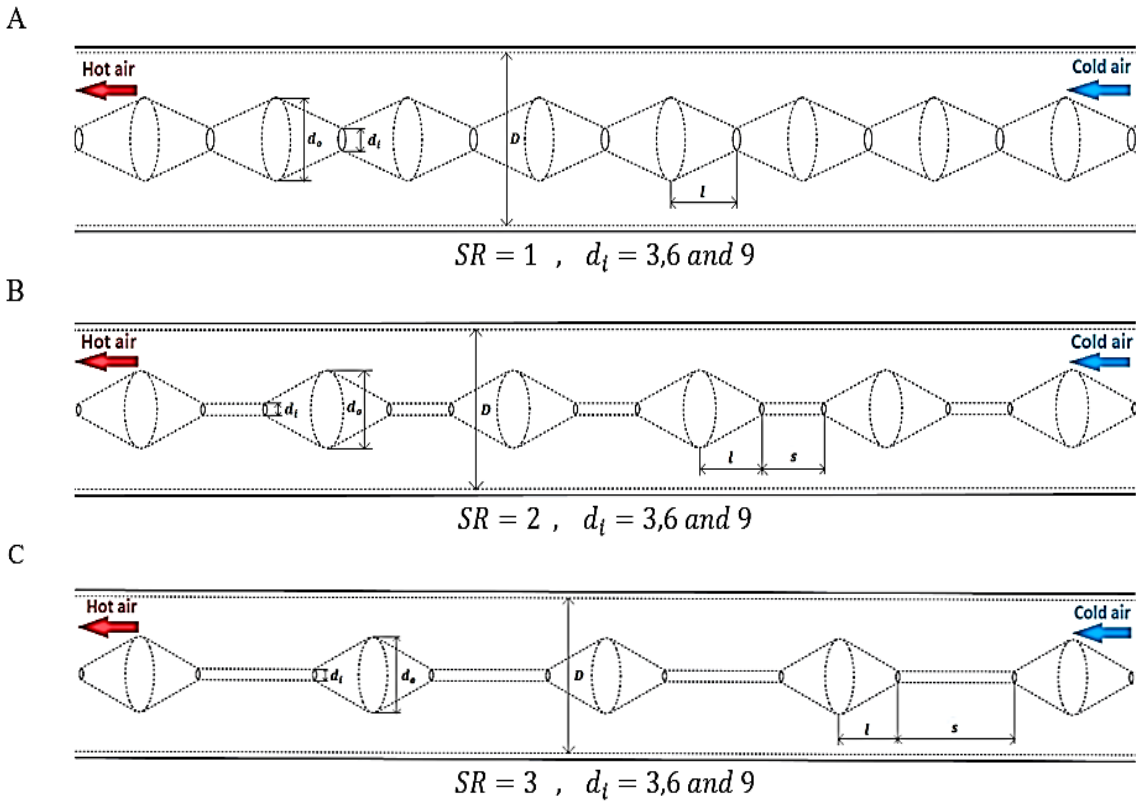

Fig. 2. Details of studied test tube with DST for different step ratio: (a) SR=1, (b) SR=2 and (c) SR=3.

The continuity, momentum, and energy equations are expressed as follows respectively:

Continuity equation:

$$\frac{\partial(\rho u_i)}{\partial x_i}+\frac{\partial(\rho u_i)}{\partial x_i}=0 \tag{21}$$

Momentum equation:

$$\frac{\partial}{\partial x_i}\left(\rho u_i u_j\right)=-\frac{\partial P}{\partial x_i}+\frac{\partial}{\partial x_j}\left[\mu\left(\frac{\partial u_i}{\partial x_j}+\frac{\partial u_j}{\partial x_i}\right)\right]-\frac{2}{3}\mu\frac{\partial u_k}{\partial x_k}\delta_{ij} \tag{22}$$

Energy equation:

$$\frac{\partial}{\partial x_i}\left(\rho u_j C_P T-k\frac{\partial T}{\partial x_j}\right)=u_j\frac{\partial P}{\partial x_j}+\left[\mu\left(\frac{\partial u_i}{\partial x_j}+\frac{\partial u_j}{\partial x_i}\right)\right]-\frac{2}{3}\mu\frac{\partial u_k}{\partial x_k}\delta_{ij} \tag{23}$$

in Eqs. (20-22), μ is dynamic viscosity, k is the kinetic energy of the turbulent flow and the C_P is specific heat in constant pressure. In simulation, the solving model (K-ω, SST) is considered and the solving algorithm (SIMPLE) is considered. For input boundary conditions, the velocity inlet is used (Velocity inlet). For outlet boundary conditions, the pressure outlet condition has been used (Pressure Outlet). There is also a fixed heat flux on the surface. Air is used as the fluid in the simulation. Before numerical simulation, the grid independence test and validation should be performed. Accordingly, nine tube geometry is simulated by changing the parameters DST with the number of mesh between 300,000 and 8,000,000, and the results are calculated by analysis (CFD). The triangular mesh image in part of the geometry studied is shown in Fig. 3.

After verifying the numerical solution of the present work, the Nusselt number (Nu) of this study is compared to the results of both plain tubes [26] and tubes with DST which was presented by Eiamsa-ard and Promvonge [20]. The current validation of this study with experimental study Eamesa-ard and Promvonge has been carried out at the angle of 45 ° and the tail length ratio of the unit was compared. Accordingly, deviation between the numerical results (present work) and theoretical data is considered to be in a reasonable range. The maximum deviation is 12%. The numerical results obtained in the analysis of CFD, heat transfer coefficient, Nusselt number and friction factor for DST in tube side for steps $(SR = 1{,}2\ and\ 3)$ and diameters $(d_i = 3{,}6\ and\ 9\ mm)$ by the nonlinear regression is calculated as the relations (21), (22) and (23):

$$h_{t,DST}=\left(k_t/d_t\right)0.160Re_{t,DST}^{\ 0.621}SR_{t,DST}^{\ -0.086}\left(\frac{d_i}{d_o}\right)_{t,DST}^{-0.026}Pr_t^{0.4} \tag{24}$$

$$Nu_{t,DST}=0.160Re_{t,DST}^{\ 0.621}SR_{t,DST}^{\ -0.086}\left(\frac{d_i}{d_o}\right)_{t,DST}^{-0.026}Pr_t^{0.4} \tag{25}$$

$$f_{t,DST}=2.156Re_{t,DST}^{\ -0.287}SR_{t,DST}^{\ -0.366}\left(\frac{d_i}{d_o}\right)_{t,DST}^{-0.234} \tag{26}$$

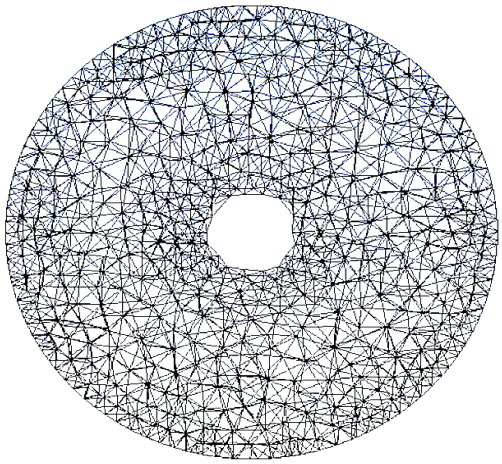

Fig. 3. Grid in the cross-sectional plane at x = 0.25 m in the tube.

3. Design parameters and objective functions

Nine optimal design variables for the present study are tube arrangement, tube diameter, tube step ratio, tube length, tube number, baffle distance ratio, baffle cut ratio, turbulator step ratio and turbulator internal rod diameter. The range of variables and their steps are shown in Table (1). Thermal

efficiency and total cost, which involving the investment cost and the operating cost for energy pumping, are considered as objective functions.

$$C_{total} = C_{in} + C_{op} \tag{27}$$

The shell and tube cost of stainless steel is calculated as. In which A_t is the total surface heat transfer outside the tube [28]:

$$C_{in} = 8500 + 409 A_t^{0.85} \tag{28}$$

The operating cost for energy pumping and overcoming friction in both hot and cold flows has been calculated as (27) [29]. Where ny lifetime of equipment during the year, i interest rate, K_{el} price of electrical energy, τ hours of operation per year, and η pump efficiency.

$$C_{op} = \sum_{k=1}^{ny} \frac{C_o}{(1+i)^k} \tag{29}$$

$$C_o = PK_{el}\tau \tag{30}$$

$$P = \frac{1}{\eta_p}\left(\frac{m_t}{\rho_t}\Delta p_t + \frac{m_s}{\rho_s}\Delta p_s\right) \tag{31}$$

4. Case study

The initial values and characteristics STHE studied are as follows. The flow of oil (hot stream, $(hot\ stream, C_p = 2115\ j/kg\ K)$ is entered with a mass flow rate of 4.5 kg/s and an input temperature of $351.45\,k$ from the shell side. The flow of water $(Cold\ stream, C_p = 4120\ j/kg\ K)$ is entered with a entered with a mass flow rate of $1.1\ kg/s$ and an input temperature of $303.15\,k$ the tube side. Table 2 describes the thermophysical conditions and characteristics of hot and cold sections. Lifetime of the equipment $(ny = 10\ yr)$ is 10 years. The interest rate (i) is 10%, the electrical energy price (K_{el}) is $0.15\ \$/Kwh$, the operating hours per year $(\tau = 7500\ h/yr)$, and the pump efficiency $(\eta = 0.6)$. Three arrangement tubes of 30, 45 and 90 degrees were used in this study. Also, 20 standard arrangement and according to the inner and outer diameter of the tube are given in Table (3) [28].

Table 1. Design parameters range

Variables	From	To
Tube arrangement	30, 45 and 90°	-
Tube inside diameter(m)	0.0112	0.0153
Pt/Do	1.25	2
Tube length(m)	3	8
Tube number	100	600
Baffle cut ratio	0.19	0.32
Baffle spacing ration	0.2	1.4
SR	1	3
DI	3	9

Table 2. STHE operating conditions

Thermophysical properties and process data	Shell side (hot stream) Oil	Tube side (cold stream) Water
Density (kg/m3)	860	995
Specific heat (J/kg K)	2115	4120
Viscosity (kg/m s)	0.0643	0.000695
Thermal conductivity (W/m K)	0.14	0.634
Fouling factor (W/K)	0.00015	0.000074

Table 3. Internal and external diameters data (di, do) in inches for 20 standard tubes.

0.444, 1/2	0.407, 5/8	0.435, 5/8	0.481, 5/8
0.495, 5/8	0.509, 5/8	0.527, 5/8	0.541, 5/8
0.555, 5/8	0.482, 3/4	0.510, 3/4	0.532, 3/4
0.560, 3/4	0.584, 3/4	0.606, 3/4	0.620, 3/4
0.634, 3/4	0.352, 3/4	0.680, 3/4	0.607, 7/8

Table 4. The optimal values of objective functions for design points A to E on Pareto-optimal fronts curve

	A	*B*	*C*	*D*	*E*
Effectiveness	0.69	0.66	0.60	0.51	0.40
Total Cost ($)	20500	17400	14800	12900	12200

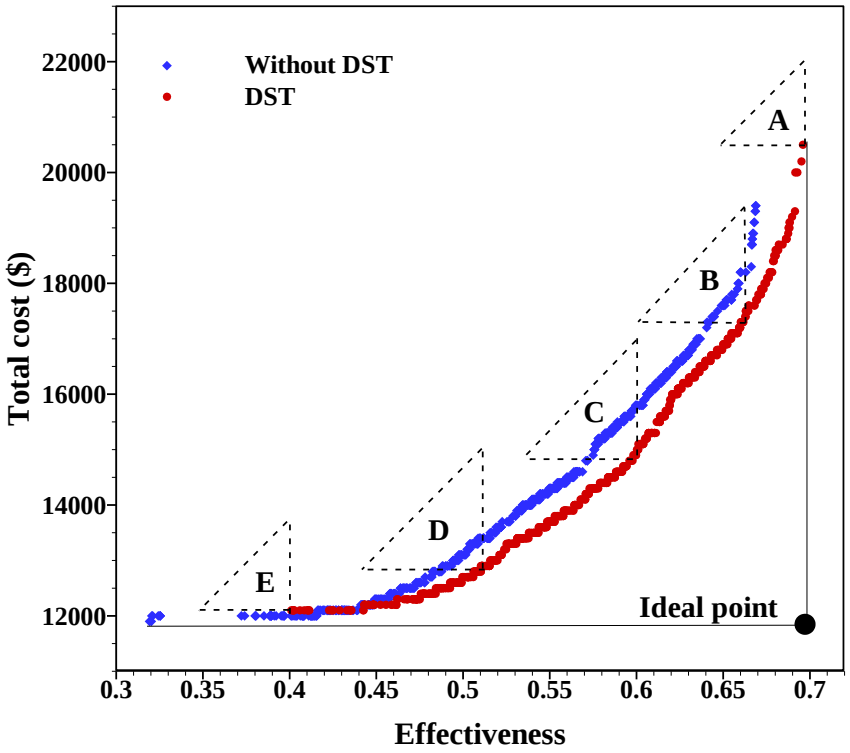

Fig. 4. The distribution of Pareto-optimal points solutions using NSGA-II.

5. Discussion and results

5.1. Optimization results

Of Nine optimal design variables for the present study which including tube arrangement, tube diameter, tube step ratio, tube length, tube number, baffle distance ratio, baffle cut ratio, turbulator step ratio and turbulator internal rod diameter used for maximize Efficiency and minimizing the total cost. The number of generations 1000, the number of repeat 100, the crossover probability of $P_C = 0.9$, gene mutation probability of $P_m = 0.035$ and controlled elitism value $c = 0.65$.The pareto diagram, which include Pareto optimal solutions', is shown in Fig. 4. This figure shows the variation in thermal efficiency versus to the total cost. The optimal design STHE requires multi-objective optimization techniques. In Fig. 4, the distribution of Pareto-optimal points solutions for STHE in use mode of DST on the tube side and without using DST is shown. With increasing efficiency STHE, the total cost increases. The optimal overall cost and improved thermal efficiency STHE equipped to DST for the five sample points (A-E) is shown in Fig. 4. The highest efficiency at point A and the lowest cost at point E occurs. according on the input variables expressed in Table (1), the efficiency and total cost for the five points (A-E) are expressed in Table (4). Also, comparing the results of the Pareto-optimal points solutions with and without the use of DST, it is clear that the use of DST on the tube side improves thermal performance and reduces overall costs. For two each objective function, each of the optimal points (A-E) is premier to the Pareto-optimal points solutions for usual STHE. As shown in the figure, the range of premier of these points is represented by a triangle. For example, in point (C), which is the preferred area for optimum design STHE, the cost was reduced to ($) 1100 at 60% efficiency, in other words, the cost was

reduced by 7.5%. Also, at this point, at an expense of ($) 14,800, efficiency has improved by as much as 5.3%. also in point (B) the cost was reduced by 4.6% at 66% efficiency. Also, at this point, at an expense of ($) 17,400, efficiency has improved by as much as 3.12%. as the same way in point (D) the cost was reduced by 4.44% at 51% efficiency. Also, at this point, at an expense of ($) 12,900, efficiency has improved by as much as 6.25%. In general, the optimal point choice for two objective functions, depending on the application of engineering STHE, can be different.

5.2. Distribution of variables for pareto optimal front

In Fig. (5a-i), the optimal values of the variables are shown. Fig. 5a shows the dispersion distribution of the tube arrangement. By choosing the 30 arrangement tube, simultaneously with improving the effectiveness, costs are reduced. Eight other design parameters have a dispersion distribution in their allowed range Fig. (5b-i).

5.3. Sensitivity analysis

In Fig. 6a-g, changes in thermal performance improvement and total cost relative to design variables are shown. In Fig. 6a, with increasing pt/Do, the pipe spacing increases and the number of tubes decreases, so the total efficiency and cost will be reduced in the case with and without DST. Also, the gradient of variation is not very different in both cases. As the tube length increases (L), the heat transfer surface increases, so the efficiency and cost increase both state with and without DST Fig. 6b. In Fig. 6c, with increasing tube numbers, efficiency and cost increase for both state with and without DST, but the gradient of the change in state without DST is high, and in the other case, the gradient of the change is very low. In other words, in the state of without use of DST, with tube number changes, both objective functions increase significantly, and in other cases, changes are low. In Fig. 6-d, changes in objective functions happen with a very low gradient than BC/Di. By increasing Lbc/Di in both state with and without the use of DST, the turbulence decreases and the heat transfer decreases and the efficiency with low gradient and cost with a higher gradient decreases. Fig. 6e. This means that increasing Lbc/Di reduces the cost considerably while reducing efficiency. As shown in Fig. 6-e, in state of use DST, the total cost with Lbc/Di variations is also lower than usual STHE. In Figs (6-f and g), with increasing (SR) and (d_i/d_o), the objective functions with low gradient decrease.

5.4. Shell and tube side heat transfer coefficient ($W\,m^{-2}k^{-1}$)

In Fig. 7-a and b, the distribution of heat transfer coefficient ($\mathrm{W\,m^{-2}k^{-1}}$) versus Total cost ($) for cold and hot flows on both sides of the shell and tube is shown for the pareto optimal points. As it is evident on the shell side, the transfer heat transfer coefficient for both states with and without DST has the values that are relatively equal to the total cost. But in Fig. 7b, in the tube side with DST turbulence, increases the turbulence and the Nusselt number increases. Therefore, by improving the heat transfer near the wall on the tube side, the heat transfer coefficient values of the increased and above the usual STHE state.

5.5. Shell and tube side pressure drop (kpa)

In Figures (8-a and b), the values pressure drop (kPa) versus the total cost ($) for both sides of the shell and tube are shown for the pareto optimal points with and without DST. As shown in Fig. 8a, that the shell side pressure drop changed in the range of 1-60 kPa. Also that the shell side pressure drop changed in the range of 8-50 kPa Fig. 8b. For flow on the tube side, with increasing total cost, the amount of pressure drop has increased significantly, but on the shell side, by increasing the total cost, the drop in pressure in the range between 1-20 (kPa) has almost stabilized. On the shell side, with and without the use of DST, the value pressure drop is near to each other, but on the tube side by using DST, due to the creation of impediment in the flow direction and also the rotation of the flow, increases the friction factor, which as a result increases the pressure drop.

a

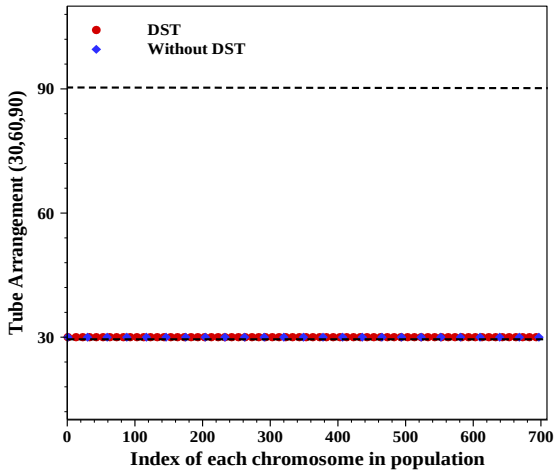
DST
Without DST
Tube Arrangement (30,60,90)
90
60
30
0
100
200
300
400
500
600
700
Index of each chromosome in population

b

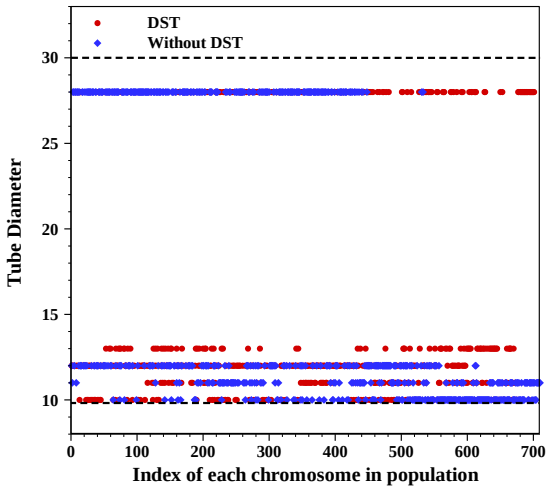
DST
Without DST
Tube Diameter
30
25
20
15
10
0
100
200
300
400
500
600
700
Index of each chromosome in population

c

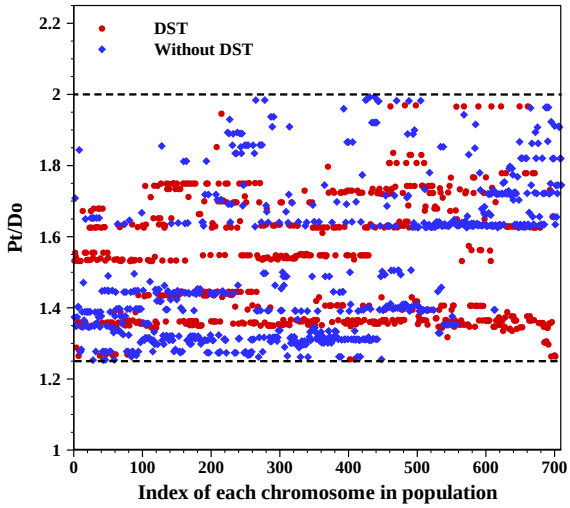
DST
Without DST
Pt/Do
2.2
2
1.8
1.6
1.4
1.2
1
0
100
200
300
400
500
600
700
Index of each chromosome in population

d

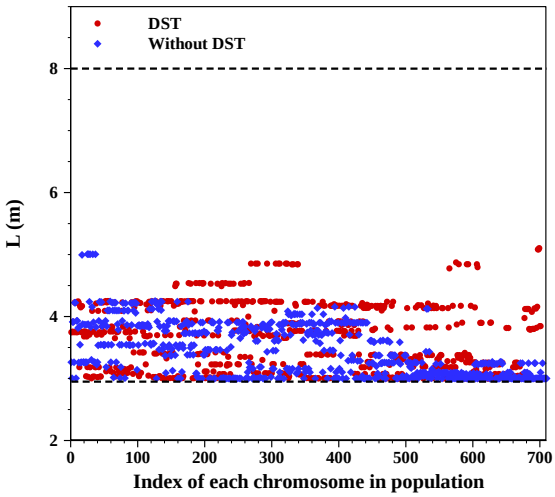
DST
Without DST
L (m)
8
6
4
2
0
100
200
300
400
500
600
700
Index of each chromosome in population

e

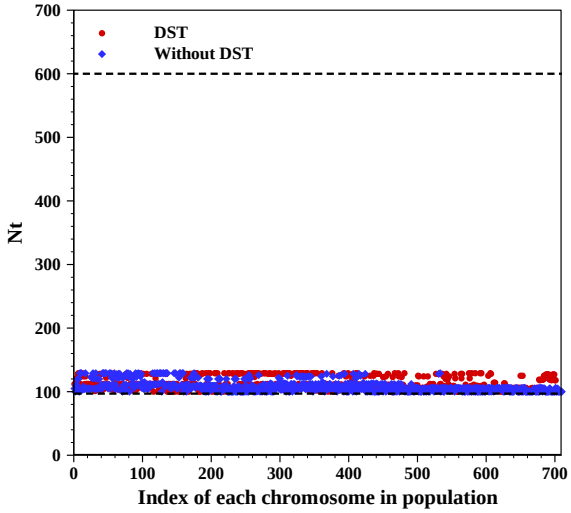
DST
Without DST
Nt
700
600
500
400
300
200
100
0
100
200
300
400
500
600
700
Index of each chromosome in population

f

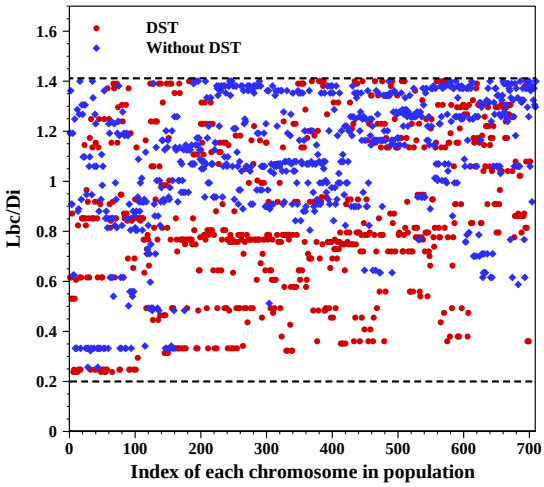
DST
Without DST
Lbc/Di
1.6
1.4
1.2
1
0.8
0.6
0.4
0.2
0
100
200
300
400
500
600
700
Index of each chromosome in population

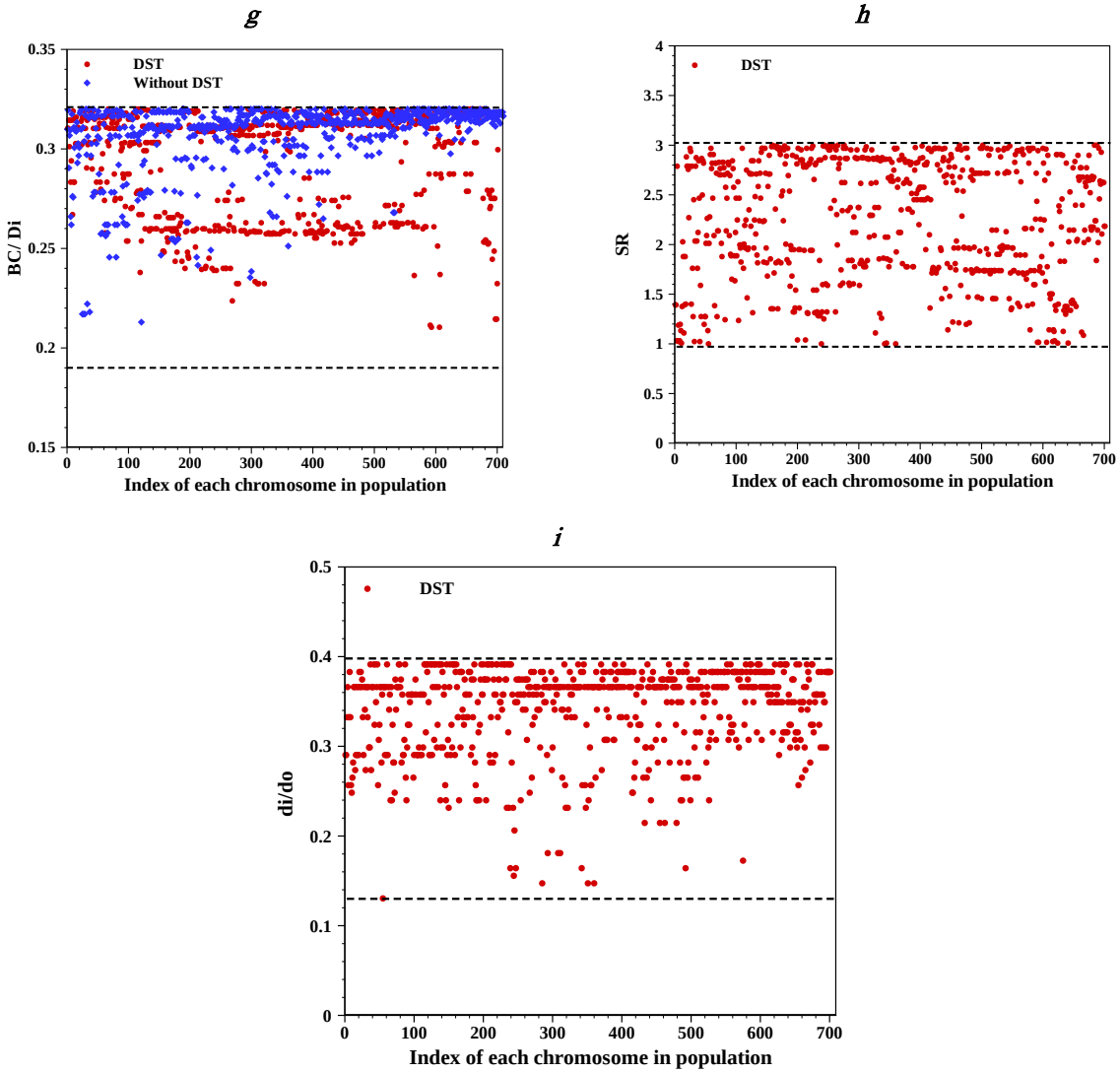

Fig. 5. Dispersion of Design variables for the Pareto optimal front : (a) tube arrangement, (b) tube diameter, (c) tube step ratio, (d) tube Length, (e) tube number (f) baffle distance ratio, (g) baffle cut ratio, (h) DST pitch ratio (SR) and (i) DST diameter of inner rod ratio (d_i/d_o).

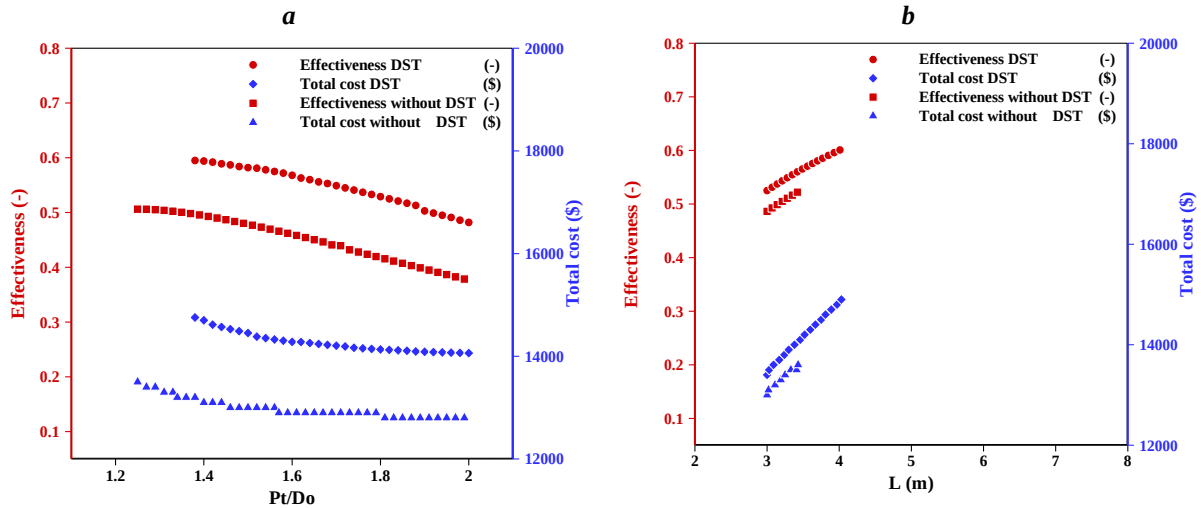

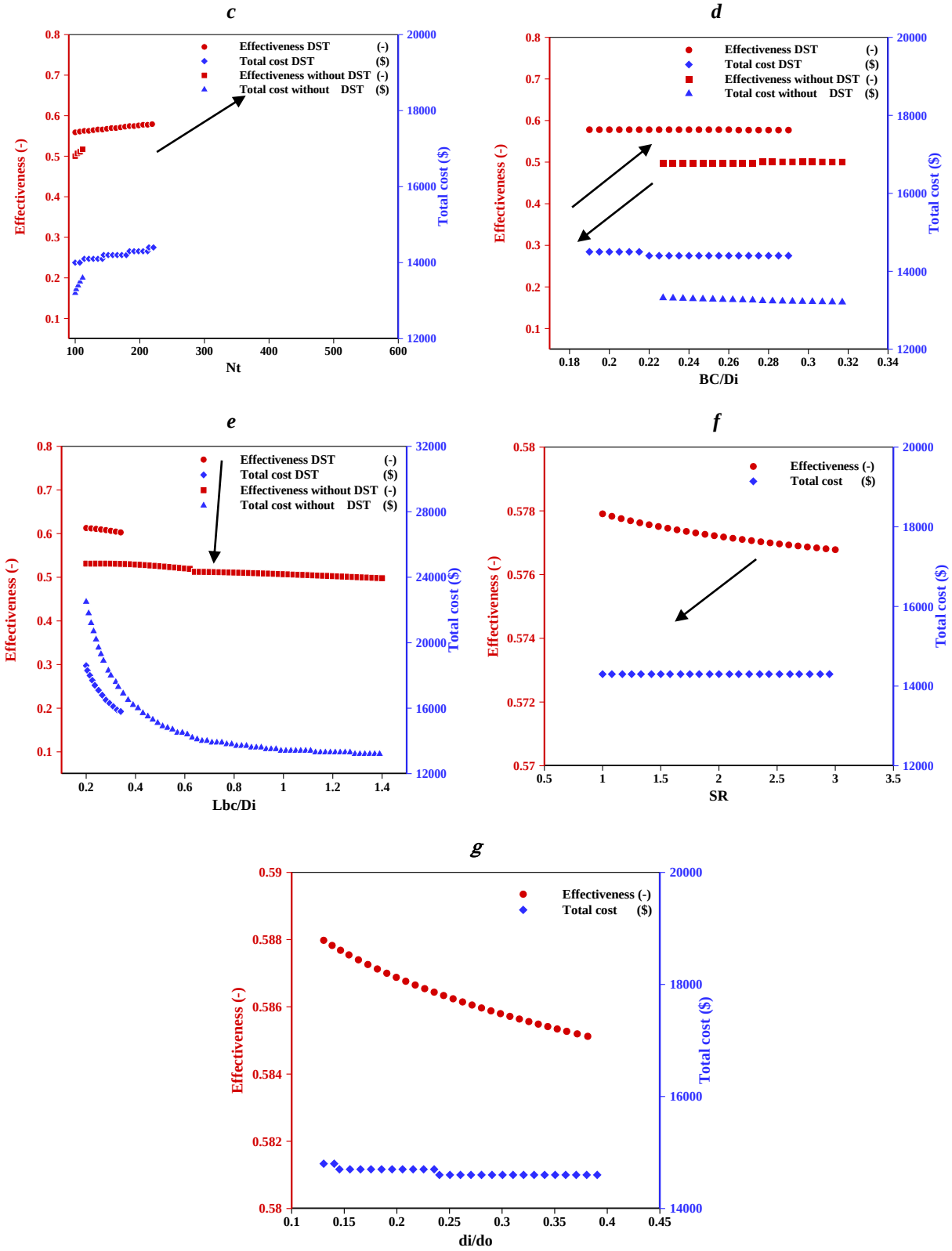

Fig. 6. Variations effectiveness and total cost ($) versus to 7 optimal design variables from area A to E: (a) tube step ratio, (b) tube Length, (c) tube number (d) baffle distance ratio, (e) baffle cut ratio, (f) DST pitch ratio (SR) and (g) DST diameter of inner rod ratio (d_i/d_o).

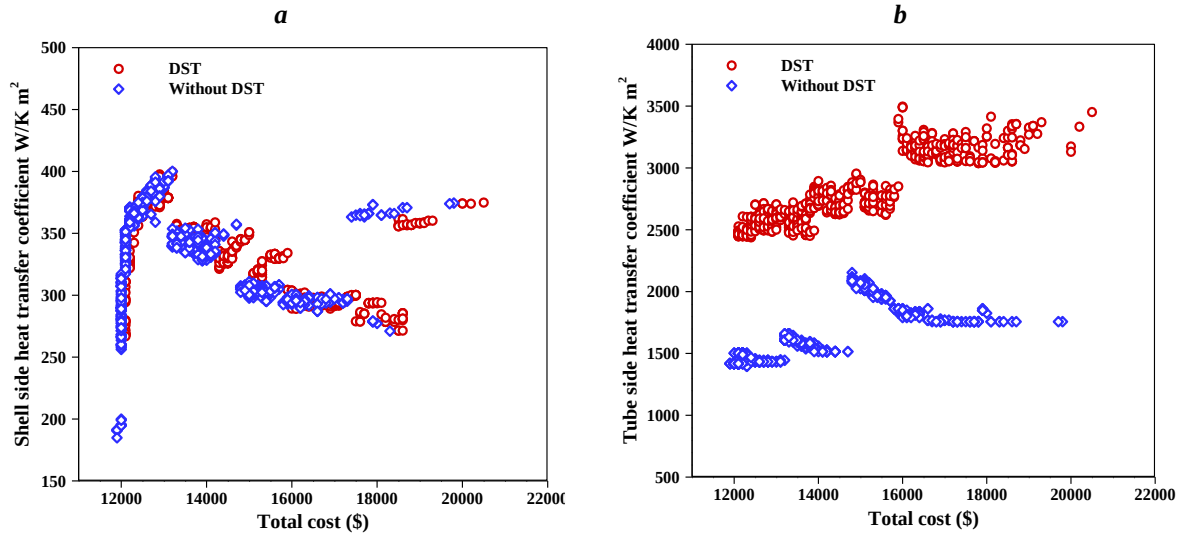

Fig. 7. Distribution of heat transfer coefficient (W $m^{-2}k^{-1}$) versus Total cost ($), (a) Shell side (b) Tube side.

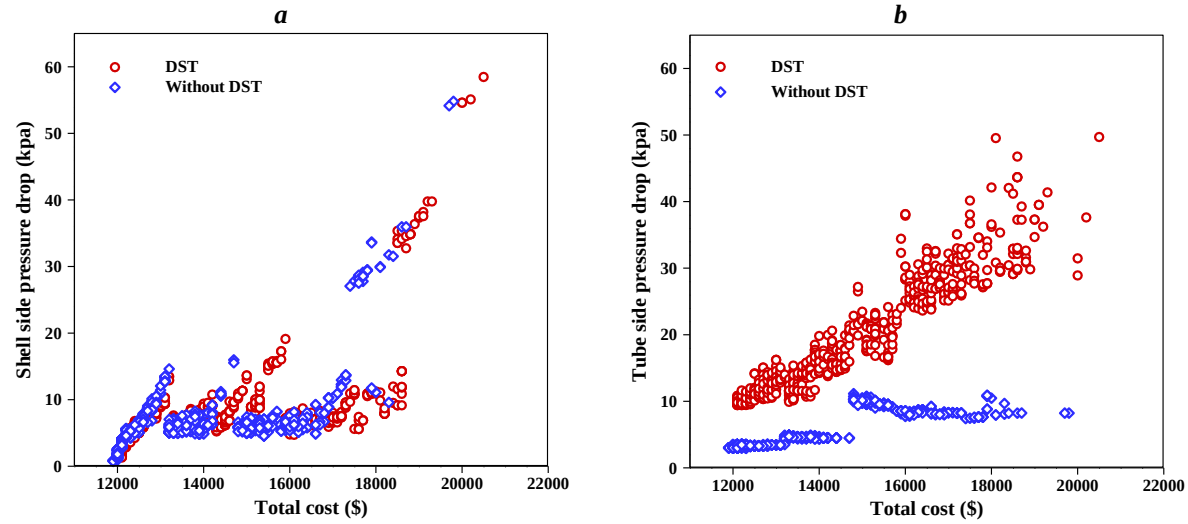

Fig. 8. Variation in pressure drop (kPa) versus the total cost ($), (a) Shell side (b) Tube side.

6. Conclusions

Thermal modeling and multi-objective optimization for STHE with a diamond-shaped turbulator has been investigated. Two factors of total cost and maximum thermal efficiency are considered as two objective functions. Nine optimal design variables for the present study are tube arrangement, tube diameter, tube step ratio, tube length, tube number, baffle distance ratio, baffle cut ratio, turbulator step ratio and turbulator internal rod diameter. The results obtained showed, the effect of optimal design parameters that caused a difference between effectiveness and overall cost. With increasing efficiency STHE, the total cost increases. The optimal overall cost and thermal efficiency improvement STHE for five sample points (A-E) has been investigated. The highest efficiency at point A and the lowest cost at point E occurs. Also Comparison of the results of the optimal Pareto optimal solutions shows that the use of turbulator DST on the tube side improves thermal performance and lower overall costs STHE compared to the non-use state. For example, in point (C), which is the preferred area for optimum design STHE, the cost was reduced to ($) 1100 at 60% efficiency, in other words, the cost was reduced by 7.5%. Also, at this point, at an expense of ($) 14,800, efficiency has improved by as much as 5.3%.

also in point (B) the cost was reduced by 4.6% at 66% efficiency. Also, at this point, at an expense of ($) 17,400, efficiency has improved by as much as 3.12%. as the same way in point (D) the cost was reduced by 4.44% at 51% efficiency. Also, at this point, at an expense of ($) 12,900, efficiency has improved by as much as 6.25%. In general, the optimal point choice for two objective functions, depending on the application of engineering STHE, can be different.

References

[1] Akhavan-Behabadi M, Kumar R, Mohammadpour A, Jamali-Asthiani M. Effect of twisted tape insert on heat transfer and pressure drop in horizontal evaporators for the flow of R-134a. International Journal of Refrigeration. 2009;32(5):922-30.

[2] Patel V, Raja B, Savsani V, Yildiz AR. Qualitative and quantitative performance comparison of recent optimization algorithms for economic optimization of the heat exchangers. Archives of Computational Methods in Engineering. 2021;28:2881-96.

[3] Wang X, Zheng N, Liu Z, Liu W. Numerical analysis and optimization study on shell-side performances of a shell and tube heat exchanger with staggered baffles. International Journal of Heat and Mass Transfer. 2018;124:247-59.

[4] Huminic G, Huminic A. Application of nanofluids in heat exchangers: A review. Renewable and Sustainable Energy Reviews. 2012;16(8):5625-38.

[5] Master BI, Chunangad KS, Boxma A, Kral D, Stehlik P. Most frequently used heat exchangers from pioneering research to worldwide applications. Heat Transfer Engineering. 2006;27(6):4-11.

[6] Bhutta MMA, Hayat N, Bashir MH, Khan AR, Ahmad KN, Khan S. CFD applications in various heat exchangers design: A review. Applied Thermal Engineering. 2012;32:1-12.

[7] Ibrahim E. Augmentation of laminar flow and heat transfer in flat tubes by means of helical screw-tape inserts. Energy Conversion and Management. 2011;52(1):250-7.

[8] Heydari O, Miansari M, Arasteh H, Toghraie D. Optimizing the hydrothermal performance of helically corrugated coiled tube heat exchangers using Taguchi's empirical method: energy and exergy analysis. Journal of Thermal Analysis and Calorimetry. 2021;145:2741-52.

[9] Solano J, García A, Vicente P, Viedma A. Flow field and heat transfer investigation in tubes of heat exchangers with motionless scrapers. Applied Thermal Engineering. 2011;31(11-12):2013-24.

[10] Barros JJC, Coira ML, de la Cruz López MP, del Caño Gochi A. Sustainability optimisation of shell and tube heat exchanger, using a new integrated methodology. Journal of Cleaner Production. 2018;200:552-67.

[11] Gu X, Wang M, Liu Y, Wang S. Multi-parameter optimization of shell-and-tube heat exchanger with helical baffles based on entransy theory. Applied Thermal Engineering. 2018;130:804-13.

[12] Wen J, Gu X, Wang M, Wang S, Tu J. Numerical investigation on the multi-objective optimization of a shell-and-tube heat exchanger with helical baffles. International Communications in Heat and Mass Transfer. 2017;89:91-7.

[13] Wang S, Xiao J, Wang J, Jian G, Wen J, Zhang Z. Configuration optimization of shell-and-tube heat exchangers with helical baffles using multi-objective genetic algorithm based on fluid-structure interaction. International Communications in Heat and Mass Transfer. 2017;85:62-9.

[14] Tharakeshwar T, Seetharamu K, Prasad BD. Multi-objective optimization using bat algorithm for shell and tube heat exchangers. Applied Thermal Engineering. 2017;110:1029-38.

[15] Rao RV, Saroj A. Economic optimization of shell-and-tube heat exchanger using Jaya algorithm with maintenance consideration. Applied Thermal Engineering. 2017;116:473-87.

[16] Mohanty DK. Application of firefly algorithm for design optimization of a shell and tube heat exchanger from economic point of view. International Journal of Thermal Sciences. 2016;102:228-38.

[17] Sadeghzadeh H, Ehyaei M, Rosen M. Techno-economic optimization of a shell

and tube heat exchanger by genetic and particle swarm algorithms. Energy Conversion and Management. 2015;93:84-91.

[18] Hajabdollahi H, Ahmadi P, Dincer I. Thermoeconomic optimization of a shell and tube condenser using both genetic algorithm and particle swarm. International journal of refrigeration. 2011;34(4):1066-76.

[19] Sanaye S, Hajabdollahi H. Multi-objective optimization of shell and tube heat exchangers. Applied Thermal Engineering. 2010;30(14-15):1937-45.

[20] Eiamsa-ard S, Promvonge P. Thermal characterization of turbulent tube flows over diamond-shaped elements in tandem. International Journal of Thermal Sciences. 2010;49(6):1051-62.

[21] Naphon P. Heat transfer and pressure drop in the horizontal double pipes with and without twisted tape insert. International Communications in Heat and Mass Transfer. 2006;33(2):166-75.

[22] Pourahmad S, Pesteei S. Effectiveness-NTU analyses in a double tube heat exchanger equipped with wavy strip considering various angles. Energy Conversion and Management. 2016;123:462-9.

[23] Rao RV, Saroj A, Ocloń P, Taler J. Design optimization of heat exchangers with advanced optimization techniques: a review. Archives of computational methods in engineering. 2020;27:517-48.

[24] Saldanha WH, Arrieta FRP, Soares GL. State-of-the-art of research on optimization of shell and tube heat exchangers by methods of evolutionary computation. Archives of Computational Methods in Engineering. 2021;28:2761-83.

[25] Shah RK, Sekulic DP. Fundamentals of heat exchanger design: John Wiley & Sons; 2003.

[26] Bergman TL. Fundamentals of heat and mass transfer: John Wiley & Sons; 2011.

[27] Kakaç S, Liu H, Pramuanjaroenkij A. Heat exchangers: selection, rating, and thermal design:CRC press; 2002.

[28] Standards of the Tubular Exchanger Manufactures Association, seventh ed..TEMA, Tarrytown, NY, 1998.

[29] Caputo AC, Pelagagge PM, Salini P. Heat exchanger design based on economic optimisation. Applied thermal engineering. 2008;28(10):1151-9..